

RESEARCH ARTICLE

CD44 regulates dendrite morphogenesis through Src tyrosine kinase-dependent positioning of the Golgi

Anna Skupien¹, Anna Konopka¹, Pawel Trzaskoma¹, Josephine Labus², Adam Gorlewicz¹, Lukasz Swiech³, Matylda Babraj¹, Hubert Dolezyczek¹, Izabela Figiel⁴, Evgeni Ponimaskin², Jakub Wlodarczyk⁵, Jacek Jaworski³, Grzegorz M. Wilczynski¹ and Joanna Dzwonek^{1,*}

ABSTRACT

The acquisition of proper dendrite morphology is a crucial aspect of neuronal development towards the formation of a functional network. The role of the extracellular matrix and its cellular receptors in this process has remained enigmatic. We report that the CD44 adhesion molecule, the main hyaluronan receptor, is localized in dendrites and plays a crucial inhibitory role in dendritic tree arborization *in vitro* and *in vivo*. This novel function is exerted by the activation of Src tyrosine kinase, leading to the alteration of Golgi morphology. The mechanism operates during normal brain development, but its inhibition might have a protective influence on dendritic trees under toxic conditions, during which the silencing of CD44 expression prevents dendritic shortening induced by glutamate exposure. Overall, our results indicate a novel role for CD44 as an essential regulator of dendritic arbor complexity in both health and disease.

KEY WORDS: CD44, Golgi fragmentation, Src kinase, Dendritic arborization, Extracellular matrix

INTRODUCTION

Dendritic arborization patterns define neuronal subtypes and have important functional implications, determining how signals that come from individual synapses are integrated (Segev and London, 2000; Gullledge et al., 2005; Koleske, 2013). The complexity of dendritic trees and their functional capabilities are altered in various psychiatric and neurodevelopmental disorders, such as schizophrenia, Down's syndrome, fragile X syndrome, Angelman's syndrome, Rett's syndrome and autism (Kaufmann and Moser, 2000; Jan and Jan, 2010; Kulkarni and Firestein, 2012). Developing dendrites are responsive to extrinsic signals that are mediated by secreted proteins, their receptors and some adhesion molecules (Urbanska et al., 2008; Jan and Jan, 2010). An important part of the extracellular environment is the extracellular matrix (ECM). Its receptors and the molecular

mechanisms of signal transduction from the ECM to neuronal cells that are involved in morphogenetic processes are still poorly understood.

The main component of the ECM in the brain is hyaluronan, a ubiquitous linear polymer of glycosaminoglycans (Novak and Kaye, 2000). The major receptor for hyaluronan is CD44, a multifunctional glycoprotein that mediates cell–cell and cell–matrix adhesion, cell migration and signaling (Ponta et al., 2003). The bulk of the literature that describes CD44 function comes from cancer studies, in which CD44–hyaluronan binding is thought to play a key role in the regulation of tumor cell migration (Ponta et al., 2003). The molecule provides a link between the plasma membrane and actin cytoskeleton (Martin et al., 2003; Bourguignon, 2008). Based on studies in non-neuronal cells, CD44 can be regarded as a key molecule that transduces signals from the ECM into the cell, influences various intracellular signaling cascades and changes cell behavior. By contrast, the function and mechanisms of action of CD44 in neuronal cells are not well established.

CD44 is expressed in both the peripheral and central nervous system (CNS). Originally, CD44 expression in the brain was reported to occur exclusively in glial cells (Girgah et al., 1991; Vogel et al., 1992; Moretto et al., 1993; Sherman et al., 2000; Bouvier-Labit et al., 2002; Gorlewicz et al., 2009). However, several subsequent reports have demonstrated the neuronal expression of this molecule in human brain sections (Kaaijk et al., 1997), embryonic optic chiasm neurons (Sretavan et al., 1994) and facial motoneurons (Jones et al., 1997). Recently, CD44 mRNA has been detected in neurons in the striatum, extended amygdala and certain hypothalamic, cortical and hippocampal regions of the forebrain (Glezer et al., 2009). Moreover, it has been found in the central respiratory control system within the brain stem (Matzke et al., 2007) and granule neurons in the adult cerebellum (Naruse et al., 2013).

The neuronal function of CD44 remains to be elucidated, although some evidence indicates that CD44 might be involved in axon guidance during neuronal development (Sretavan et al., 1994; Lin and Chan, 2003; Ries et al., 2007). Additionally, CD44 was suggested to act as a co-receptor for receptor tyrosine kinases and serve as a site for signaling molecule assembly (Sherman et al., 2000; Orian-Rousseau et al., 2002; Matzke et al., 2007; Gorlewicz et al., 2009). Recently, CD44 in sensory neurons has been described to inhibit plasma membrane Ca²⁺ adenosine triphosphatase (PMCA) through the activation of Src family kinases (SFKs, Lck, Fyn; Ghosh et al., 2011). The lack of CD44 in pre-Böttinger complex interneurons within the brain stem was also shown to reduce glutamatergic synaptic excitation *in vivo* (Matzke et al., 2007). In conclusion, although the amount of data

¹Laboratory of Molecular and Systemic Neuromorphology, Nencki Institute of Experimental Biology, Polish Academy of Sciences, Pasteura 3, 02-093 Warsaw, Poland. ²Cellular Neurophysiology, Center of Physiology, Hannover Medical School, 30625 Hannover, Germany. ³Laboratory of Molecular and Cellular Neurobiology, International Institute of Molecular and Cell Biology, Trojdena 4, 02-190 Warsaw, Poland. ⁴Laboratory of Neurobiology, Nencki Institute of Experimental Biology, Polish Academy of Sciences, Pasteura 3, 02-093 Warsaw, Poland. ⁵Laboratory of Cell Biophysics, Nencki Institute of Experimental Biology, Polish Academy of Sciences, Pasteura 3, 02-093 Warsaw, Poland.

*Author for correspondence (j.dzwonek@nencki.gov.pl)

on neuronal CD44 function is increasing, our understanding of its function is far from being comprehensive.

In the present study, we describe the developmental regulation of CD44 in postnatal brain and uncover dendrites as a major site of its fine-structural localization. To gain further insights into the physiological roles of CD44 in neurons, we examined the consequences of neuronal knockdown of CD44 *in vitro* and *in vivo*. Our results show that the loss of CD44 results in an increase in the complexity of dendritic arbors in hippocampal neurons cultured *in vitro* and cortical neurons electroporated *in vivo*. Moreover, the knockdown of CD44 results in structural alteration of the Golgi, an organelle that is essential for mediating dendritic polarity, growth and maintenance. We found that CD44 interacts with Src kinase in the brain, and the activation of both c-Src and its main substrate, focal adhesion kinase (FAK), is decreased upon CD44 knockdown. The effects of CD44 knockdown on the morphology of both the Golgi and dendritic trees are blocked by the expression of a constitutively active mutant of Src kinase (Y527F), demonstrating that this kinase acts as a downstream effector of the CD44-induced signaling cascade. Additionally, the observed changes in Golgi morphology depend on actin cytoskeleton dynamics. Moreover, we show that the silencing of CD44 expression during the early development of neuronal cells exerts a significant protective effect on young neurons that are exposed to subtoxic conditions, acting to prevent dendritic shortening induced by glutamate exposure. Therefore, CD44 might be a novel therapeutic target in neurological disorders in which alterations in dendritic tree arborization have been observed.

RESULTS

CD44 is present in dendrites of pyramidal neurons throughout development

To specify the spatial and temporal expression pattern of CD44 protein in the rat brain, we investigated its expression during postnatal development. Immunohistochemistry in hippocampal sections showed the highest expression during the first days after birth [postnatal day 0–10 (P0–P10)], with a reduction observed on day 14 onwards (Fig. 1A). The CD44 signal was arranged in a distinctive honeycomb pattern around MAP-2-positive neurons but did not appear to colocalize with glial fibrillary acidic protein (GFAP)-positive astrocytic protrusions. Western blot analysis of protein extracts from rat hippocampi and cerebral cortices that were collected at different time points during development [embryonic day 18 (E18) to P60] confirmed that the expression of CD44 protein increased on the first postnatal days, peaked on days 7–10 in the hippocampus and days 10–20 in the cortex, and then decreased (Fig. 1B).

To determine whether the CD44 signal that surrounds MAP-2 immunoreactivity reflects neuronal, glial or extracellular localization of the protein, we used immunogold labeling of sections of the P10 rat hippocampus. The ultrastructural pattern of CD44 expression in the CA3 stratum radiatum was very characteristic (Fig. 1C), with 10-nm gold particles detected predominantly within dendrites (blue areas) and in association with the dendritic membrane at sites closely apposed to various structures, such as other dendritic processes or astrocyte processes (yellow areas). The quantitative analysis of the number of gold particles in dendritic profiles or dendritic plasma membranes confirmed a significant association between gold particles and these compartments compared with an expected random distribution (dendrites: $\chi^2=14.75$, $P<0.0005$;

dendritic membranes: $\chi^2=220.75$, $P<6.06\times 10^{-50}$). For the negative control, primary antibody was replaced with nonimmune immunoglobulin G (IgG). In this case, the distribution of gold particles within the dendritic profiles or at dendritic membranes did not significantly differ from the random distribution (dendrites: $\chi^2=0.038$, $P>0.05$; dendritic membranes: $\chi^2=0.025$, $P>0.05$). The characteristic timecourse of postnatal CD44 expression in the rat forebrain and the dendritic localization of the molecule led us to hypothesize about the possible role of CD44 in dendritic arborization.

CD44 regulates dendrite patterning in mammalian neurons

To determine the neuronal function of CD44, we downregulated its expression in primary hippocampal neurons using short-hairpin RNA (shRNA) constructs. We first tested the knockdown efficiency of two different shRNAs against the overexpression of rat CD44 cDNA (rCD44) in human embryonic kidney 293 (HEK-293) cells. The cells were co-transfected for 3 days with rCD44 tagged with green fluorescent protein (GFP) and either empty pSuper (control) or CD44 shRNA vectors. The β -galactosidase-coding vector was additionally included in the transfection mixture as a control for transfection efficiency. Immunoblotting (Fig. 2A) and the quantitative densitometry of protein expression (Fig. 2B) identified the most potent shRNA (#1963), which caused an effective knockdown of the rat CD44–GFP fusion protein. This particular molecule was used in the subsequent experiments.

We then tested the efficacy of this shRNA in cultured neuronal cells. Day 6 *in vitro* (DIV6) neurons were transfected with an empty pSuper or with CD44 shRNA plasmids. The plasmid that encoded GFP was added to the transfection mixture for the identification of transfected cells. At 5 days post-transfection, endogenous CD44 was detected by immunofluorescence and the intensity of immunostaining was compared. As shown in Fig. 2C,D, CD44 shRNA significantly decreased the level of endogenous neuronal CD44.

To evaluate the effect of CD44 downregulation on dendritic arbor morphology, we transfected the cells at the peak of dendritogenesis (DIV7) with pSuper/GFP or CD44 shRNA/GFP vectors and fixed them 5 days later. Tracings of neurons that are representative of all groups are presented in Fig. 3A. Morphometric analysis of the cells revealed that transfection with CD44 shRNA increased the complexity of arbor morphology (Fig. 3B–D). Specifically, transfection with CD44 shRNA increased the total dendritic length (TDL) and total number of dendritic tips (TNDTs) compared with neurons that were transfected with the pSuper plasmid (Fig. 3B,C). The Sholl analysis of neurons upon CD44 knockdown revealed an upward shift of the plot compared with the pSuper control (Fig. 3D), indicating an increase in the complexity of dendritic trees.

To confirm the specificity of the observed CD44-knockdown phenotype in neurons, we performed rescue experiments. We created a DNA construct in which silent mutations were introduced into the cDNA coding region for rCD44 (CD44Rescue), which was transcribed into mRNA that could not be recognized by shRNA. The co-expression of CD44Rescue with shRNA in neurons resulted in the re-expression of CD44 at endogenous levels (Fig. 2D) and a reversal of the knockdown-induced phenotype (Fig. 3). These data indicate that CD44-shRNA-induced changes in dendritic morphology resulted from the specific knockdown of CD44 rather than from off-target effects.

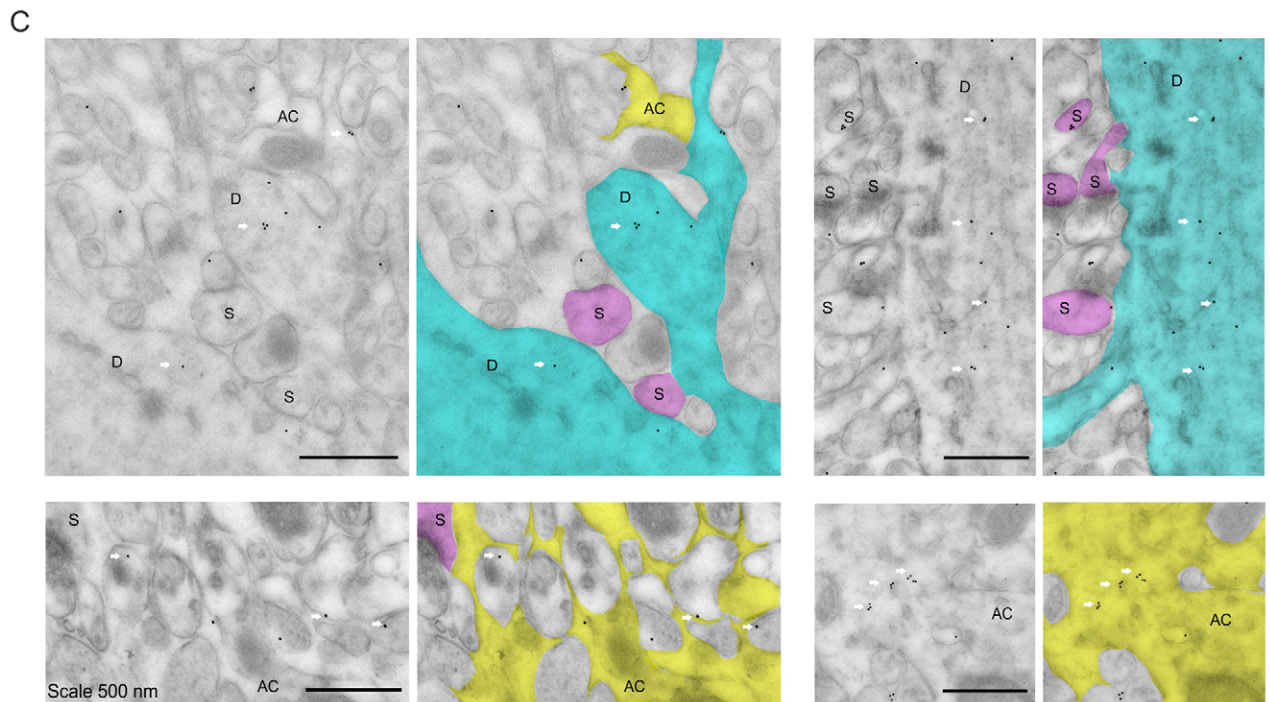
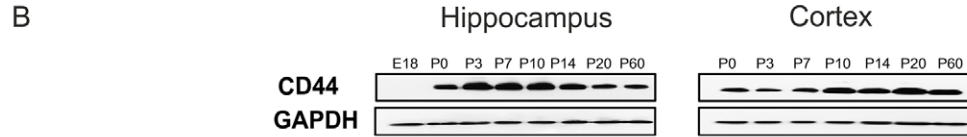
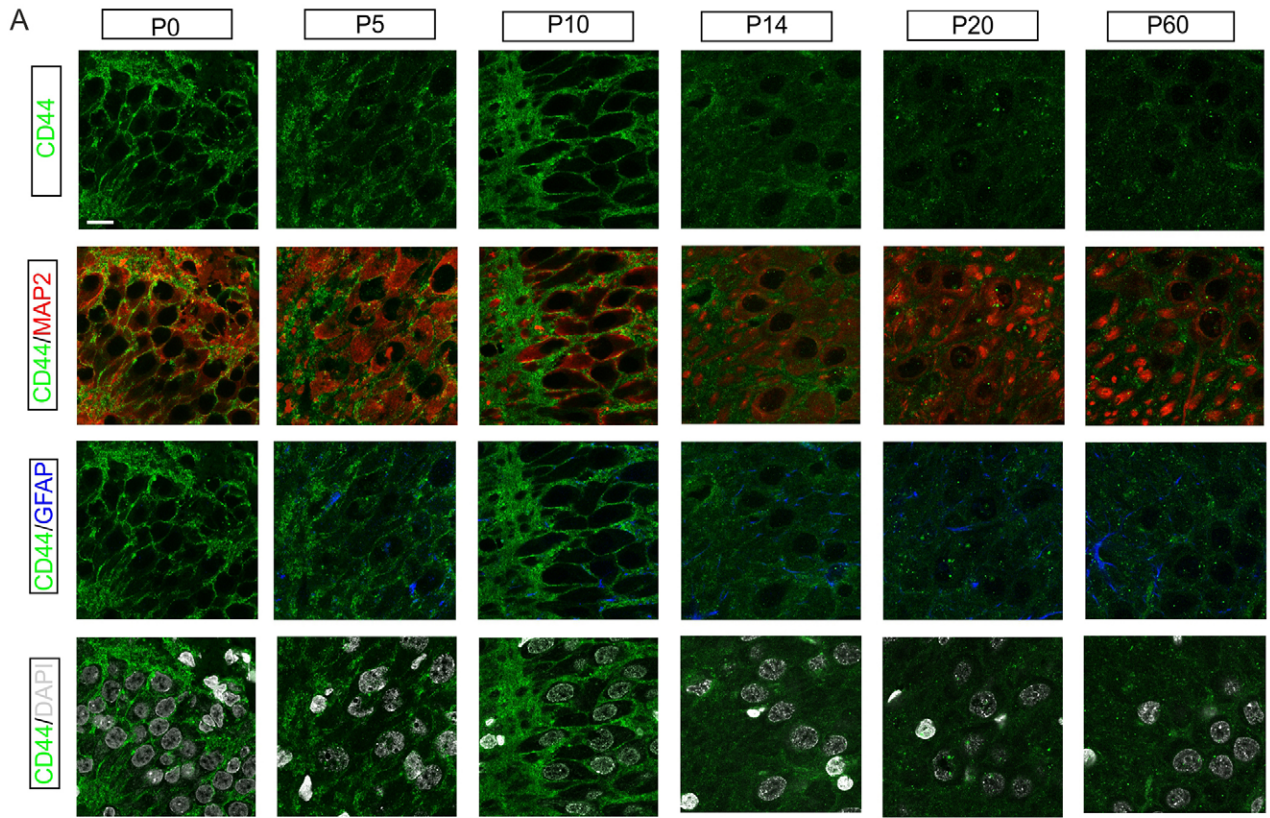


Fig. 1. See next page for legend.

Fig. 1. CD44 expression in neuronal cells is developmentally regulated. (A,B) CD44 protein expression during postnatal development of the rat hippocampus and cerebral cortex. (A) Confocal images of the CA3 region of the rat hippocampus at P0–P60, immunostained with anti-CD44 (green), anti-MAP-2 (red), anti-GFAP (blue) and DAPI (white). Scale bar: 10 μ m. (B) Immunoblot analysis of CD44 expression in the developing rat hippocampus and cerebral cortex. (C) Electron microscopic immunogold detection of CD44 in the CA3 region of the hippocampus of 10-day-old rat. Arrows point out immunogold particles indicating CD44 immunoreactivity that are present in dendrites (D, blue overlays), astrocytes (AC, yellow overlays) and dendritic spines (S, magenta overlays). $n=3$ animals per group. Scale bar: 500 nm.

To determine whether the function of CD44 in dendrite patterning is a general phenomenon that occurs in the rat brain, we performed iontoporation (iPo) to deliver the plasmid DNA into postmitotic neurons (De la Rossa et al., 2013). We introduced the plasmid DNA (pSuper or CD44 shRNA, together with GFP-coding vector) solubilized in a nuclear permeabilizing agent [*trans*-cyclohexane-1,2-diol (TCHD)] into the cerebral cortex of newborn rat pups and performed electroporation. Brains were collected and analyzed on P21. Fluorescent Nissl staining of the sections was performed to visualize cytoarchitectonics. We detected sparsely labeled neurons in the cortex (Fig. 4A). The morphometric analysis was performed exclusively on pyramidal neurons from cortical layer V. The TDL and Sholl analysis revealed that GFP-positive shRNA-transfected neurons exhibited extended dendritic arbors compared with those of control neurons (Fig. 4B,C). To examine whether there are differential effects on apical versus basal dendrites, we separately quantified the total length of apical dendrites (i.e. apical dendrite with branches; Fig. 4D), apical dendrite length (Fig. 4E), the number of apical dendrite branches (Fig. 4F), the total length of basal dendrites (Fig. 4G), the mean length of basal dendrites (Fig. 4H) and the number of basal dendrites (Fig. 4I). We found that

basal but not apical dendrite length was markedly increased in shRNA-treated neurons relative to that of control cells. Collectively, our findings suggest that CD44 regulates the patterning of dendrites throughout postnatal development.

CD44 knockdown results in Golgi dispersion

The proper structure and position of the Golgi are causally linked to dendrite morphogenesis (Horton et al., 2005; Ori-McKenney et al., 2012). Therefore, we examined the effect of CD44 knockdown on the morphology of the Golgi. Hippocampal neurons that were transfected with either pSuper- or CD44-shRNA-expressing plasmids were immunostained with the GM130 (also known as GOLGA2) cis-Golgi protein marker to assess the Golgi structure. After CD44 knockdown, we observed an increased number of smaller GM130-positive structures, suggesting Golgi fragmentation (Fig. 5A). The number of Golgi fragments per cell was higher, whereas the average volume of fragments was reduced in cells with diminished CD44 expression compared with that of controls (Fig. 5B,C). Additionally, we quantified Golgi dispersal by calculating the ratio of the total surface area of the Golgi to the total volume of the Golgi per cell. The area:volume ratios were higher for CD44-shRNA-transfected cells compared with controls (Fig. 5D). Fragmentation of the Golgi upon CD44 knockdown was rescued by co-expression of shRNA-resistant plasmid (CD44Rescue) together with CD44 shRNA. The values of the parameters that describe Golgi dispersion in CD44Rescue-transfected neurons did not significantly differ from those of control cells (Fig. 5B–D).

CD44 acts through Src kinase to regulate dendritic tree morphology

One of the molecular mechanisms of CD44 action described in different cell types is activation of the SFKs Lck, Fyn and Src

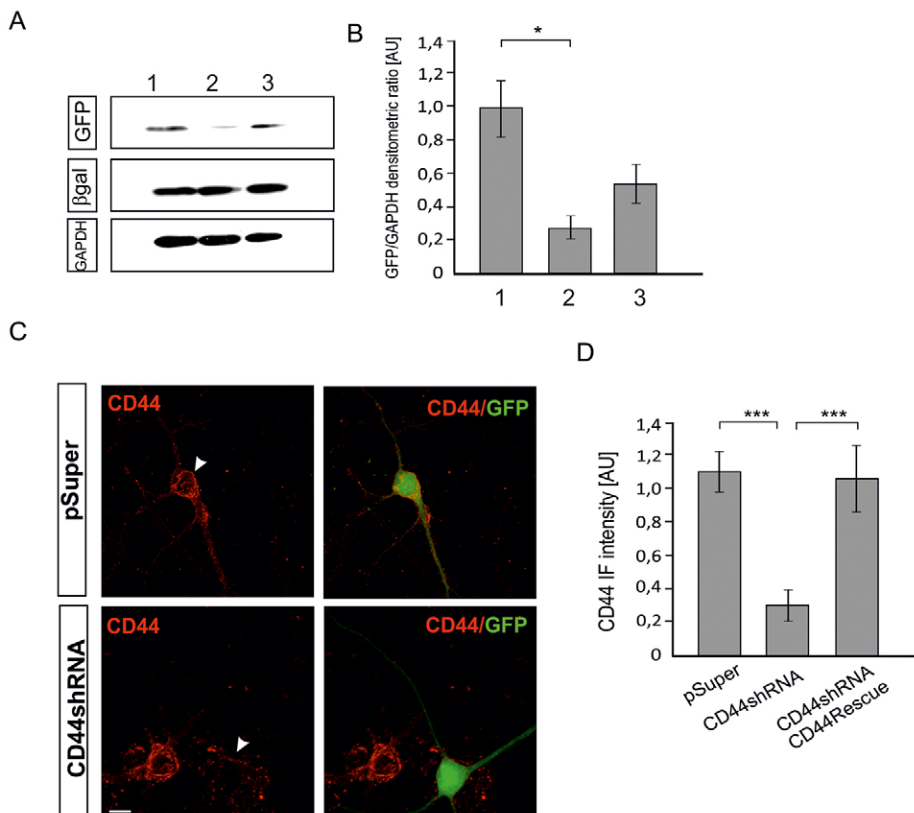


Fig. 2. CD44 shRNA effectively knocks down rat CD44 expression. (A) Immunoblot of cellular lysates of HEK293 cells co-transfected with rat CD44–GFP, β -galactosidase and pSuper (1) or CD44 shRNA #1963 (2) and #90 (3) plasmids. $n=3$ independent batches of cells. (B) Quantitative densitometry of protein expression, normalized to GAPDH. (C) Primary hippocampal neurons transfected with pSuper or CD44 shRNA plasmids together with β -actin–GFP were subjected to immunocytochemistry using the anti-CD44 antibody (red). The arrowheads indicate transfected cells. Scale bar: 10 μ m. (D) The effect of CD44 knockdown was estimated based on the average intensity of the CD44 immunofluorescence (IF) signal in transfected cells. $n=25$ neurons per group. AU, arbitrary units. Data in B,D show the mean \pm s.e.m.; * $P<0.05$; *** $P<0.001$.

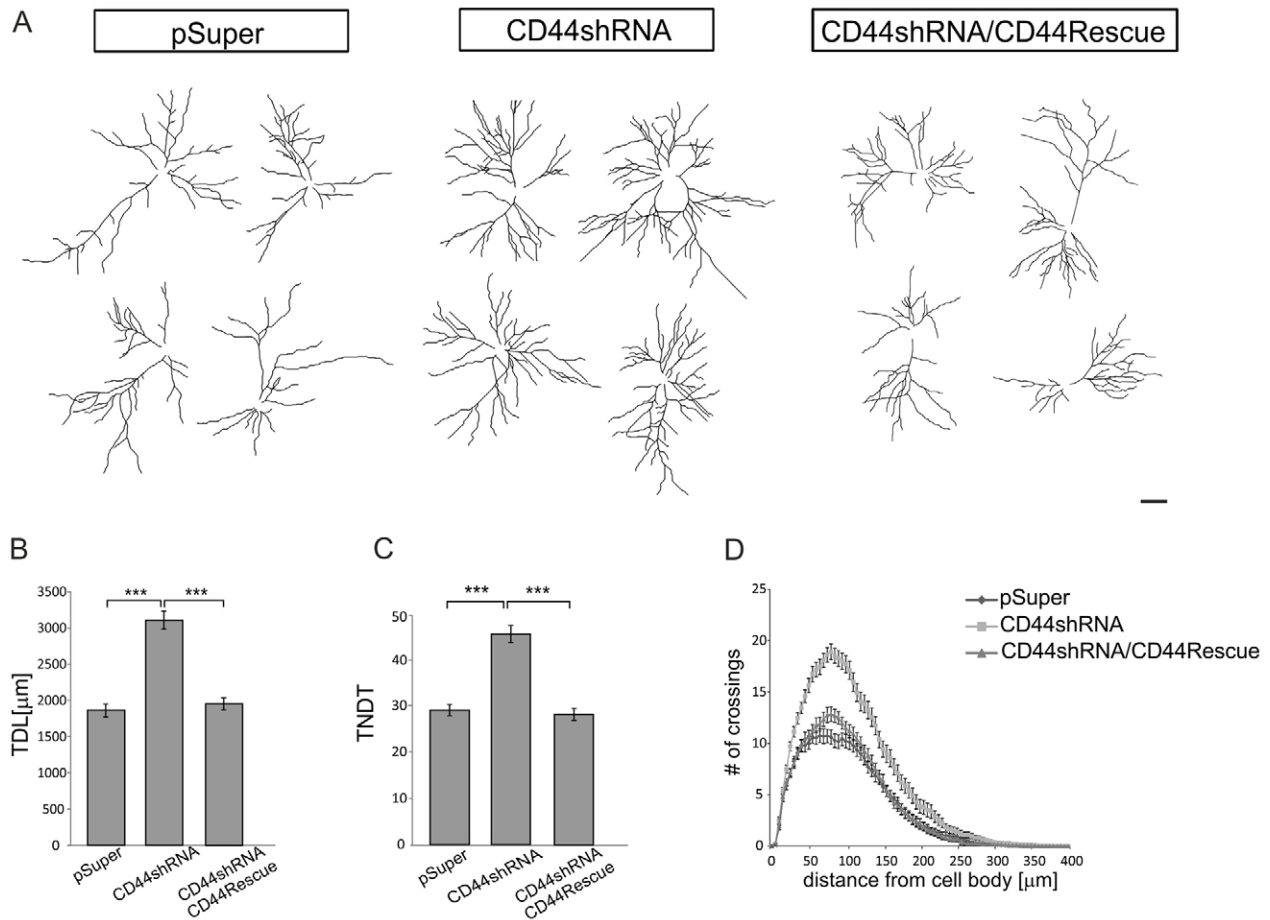


Fig. 3. Knockdown of CD44 stimulates the elaboration of dendrites of hippocampal neurons, and the effect of silencing is rescued by overexpression of an shRNA-resistant rat CD44. (A) Tracings of representative neurons co-transfected with pSuper, CD44 shRNA or CD44 shRNA/CD44Rescue together with RFP-coding vector. Scale bar: 50 μm . (B) Total dendritic length (TDL) and (C) total number of dendritic tips (TNDT) for neurons treated as in A. (D) Sholl analysis of hippocampal neurons after transfection with the indicated plasmids. At distances 25–175 μm from the cell body, the differences between CD44 shRNA and the other groups were statistically significant ($P < 0.001$). Data show the mean \pm s.e.m. ($n = 50$ neurons per group); *** $P < 0.001$.

(Ilangumaran et al., 1998; Lee et al., 2008; Ghosh et al., 2011). In breast cancer cells, the hyaluronan–CD44 interaction promotes c-Src activation (Bourguignon et al., 2010). Moreover, Src has been shown to interact directly with CD44 in tumor cells (Bourguignon et al., 2001; Lee et al., 2008), but the interaction with proteins in the brain has not yet been reported. To investigate whether CD44 directly interacts with c-Src in the rat brain, we performed immunoprecipitation with an anti-CD44 antibody followed by anti-c-Src immunoblot (Fig. 6A) using tissue homogenates from P10 rat hippocampi and cortex. Analysis of the input confirmed expression of 80-kDa CD44 and 60-kDa Src (Fig. 6A, left panel). Furthermore, we detected a band at 60 kDa after precipitation of CD44, which indicates co-precipitation of total Src (Fig. 6A). To exclude unspecific interactions, homogenates incubated with an anti-IgG isotype control were analyzed in parallel. No co-precipitation of the 60-kDa Src was detected. (Fig. 6A). These findings indicate that CD44 and c-Src kinase interact with each other in the developing rat brain. The catalytic activity of c-Src kinase requires phosphorylation at tyrosine 416. To determine whether CD44 alters the activation of c-Src, primary hippocampal neurons that were transfected on DIV5 with pSuper or CD44 shRNA plasmids were fixed at 3 days after transfection. Immunocytochemistry was performed using specific anti-pY416-Src antibody, and the

immunostaining intensity was quantified. Our results showed that the active form of c-Src was close to the membrane and in the cytoplasm in control neurons (Fig. 6B). CD44 knockdown diminished the amount of phosphorylated Src (Fig. 6B,C). One of the key Src substrates is FAK (Mitra et al., 2005). The Src-mediated phosphorylation of FAK on Tyr576 and Tyr577 promotes maximal FAK catalytic activation (Hanks et al., 2003). To determine whether CD44 alters the Src-dependent phosphorylation of FAK, we performed immunocytochemistry using specific anti-pY576-FAK antibody in control and CD44-shRNA-transfected neurons (Fig. 6D). The level of phosphorylated FAK was significantly decreased in cells with diminished CD44 expression (Fig. 6D,E).

To determine whether the function of CD44 in regulating the dendritic tree morphology described herein is also driven by Src kinase activation, we applied a plasmid that encodes the constitutively active form of Src kinase (CASrc, Y527F). We determined whether the CD44-shRNA-induced elaboration of dendritic trees in hippocampal neurons can be rescued by introducing active Src kinase into the cells. We co-transfected neurons on DIV7 with pSuper or CD44 shRNA vectors together with β -actin–GFP and a constitutively active mutant of Src kinase and fixed them 5 days later. No increase in dendritic arbor size was observed in cells that expressed CD44 shRNA together with

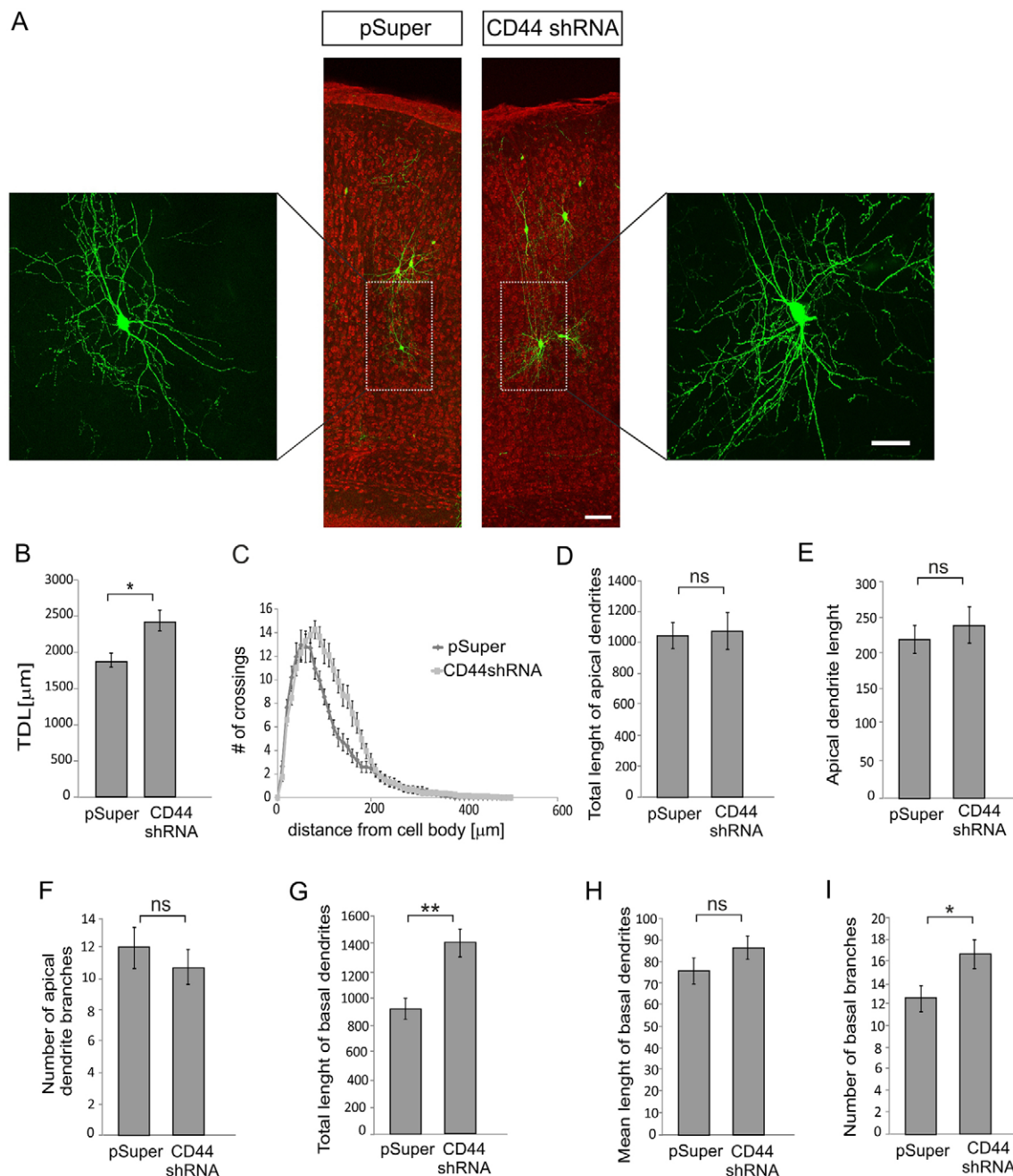


Fig. 4. CD44 regulates the development of proper dendritic morphology *in vivo*. Rat pups were electroporated *in vivo* on P0 with pSuper/GFP or CD44 shRNA/GFP plasmids and sacrificed on P21. (A) Representative images of cortical neurons are presented. The regions outlined in white are shown at higher magnification as indicated. Scale bars: 100 μm (middle panel), 50 μm (right panel). Also shown is quantitative analysis of (B) total dendritic length and (C) Sholl analysis, (D) total length of apical dendrites (apical dendrite with branches), (E) apical dendrite length, (F) number of apical dendrite branches, (G) total length of basal dendrites, (H) mean length of basal dendrites and (I) number of basal dendrites of transfected cells. Morphometric analysis was performed with 20 neurons, with 3 animals per group. In the Sholl analysis, the differences between CD44 shRNA and pSuper were statistically significant ($P < 0.01$) at distances 80–180 μm from the cell body. Data show the mean \pm s.e.m.; * $P < 0.05$; ** $P < 0.01$; ns, not significant.

the CASrc mutant (Fig. 6F–I). These results indicate that Src acts downstream of CD44 in the regulation of dendritic tree morphology.

CD44-knockdown-induced Golgi dispersion depends on Src activity and actin polymerization

To evaluate whether the effect of CD44 silencing on Golgi morphology also depends on the inhibition of Src kinase activity,

we performed morphometric analysis of the GM130-immunolabeled organelle in cells co-transfected with CD44 shRNA and CASrc (Y527F) plasmids. The effect of Golgi dispersion caused by CD44 shRNA was rescued by overexpression of the constitutively active form of Src kinase (Fig. 7A). The volume, number and area:volume ratio of the Golgi fragments in CD44 shRNA/CASrc-transfected cells did not differ significantly from that of control cells (transfected with

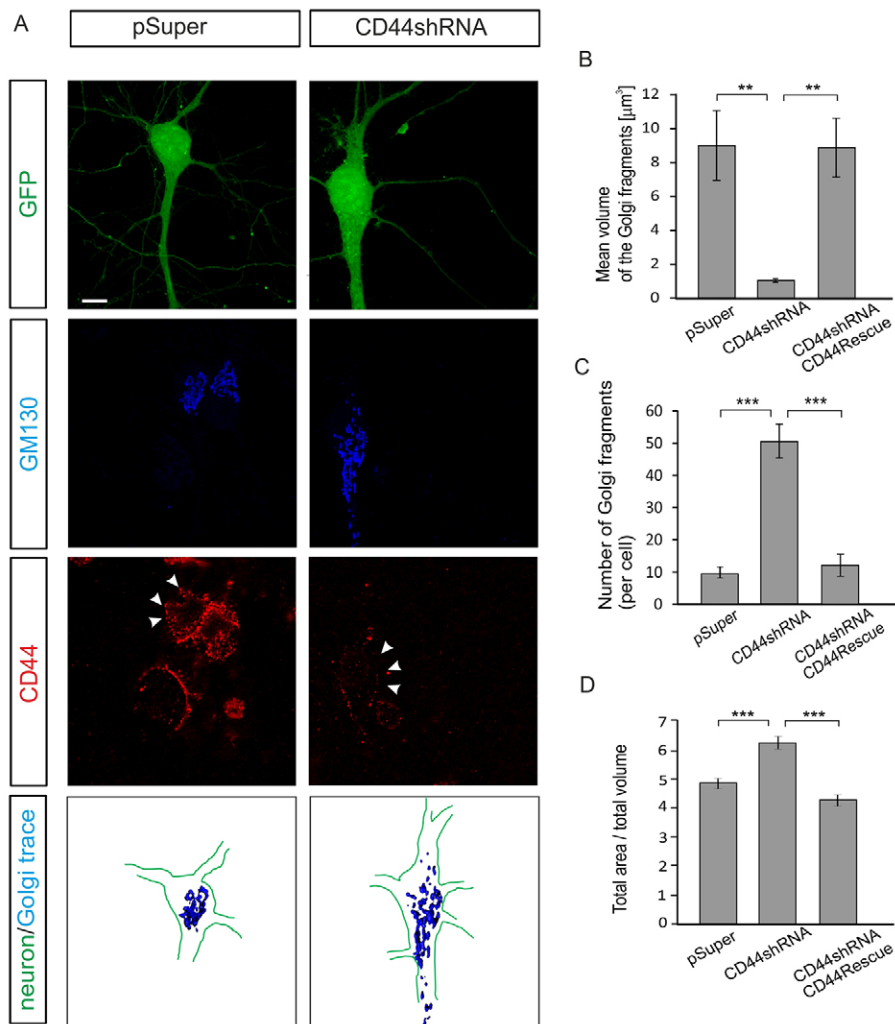


Fig. 5. Dispersion of the Golgi in neurons following CD44 knockdown. (A) Confocal images and Golgi three-dimensional reconstructions of GM130-labeled cultured hippocampal neurons transfected with pSuper or CD44 shRNA plasmids together with GFP-coding vector. After fixation, the cells were immunostained to visualize the Golgi marker GM130 (blue) and CD44 (red). Arrowheads indicate a transfected cell. Scale bar: 10 µm. (B) Quantification of the mean volume of the Golgi fragments. (C) Quantification of the number of Golgi fragments. (D) The ratio of the total surface area to total volume of the Golgi of cells transfected with pSuper, CD44 shRNA or CD44Rescue plasmids. Analyses of the Golgi of 40 cells for each experimental condition were performed. Data show the mean ± s.e.m.; ** $P < 0.01$; *** $P < 0.001$.

pSuper and GFP; Fig. 7B–D). These results indicate that Src acts downstream of CD44 in regulating neuronal Golgi morphology.

Src and FAK form an active complex that regulates actin structure through the phosphorylation of actin-binding proteins (Mitra et al., 2005). Actin cytoskeleton dynamics play an important role in the maintenance of Golgi morphology (Lázaro-Diéguez et al., 2006). We tested whether CD44-knockdown-induced Golgi fragmentation can be reversed by inhibiting actin polymerization. Neurons were transfected with pSuper or CD44 shRNA on DIV5. At 24 hours later, the cells were incubated with latrunculin B (2.5 µM) for 24 hours. Cells were fixed on DIV7 and immunostained with GM130-specific antibody. Morphometric analysis of the Golgi revealed that treatment with latrunculin B blocked Golgi fragmentation induced by CD44 knockdown (Fig. 7A–D). Therefore, actin polymerization is required for CD44-knockdown-induced dispersal of the Golgi and constitutes a potential mechanism by which Src activity regulates Golgi morphology.

CD44 silencing partially protects young hippocampal neurons from glutamate-evoked reduction of dendritic outgrowth

The treatment of young pyramidal neuronal cultures with a low concentration of glutamate has previously been shown to lead to a reduction in dendritic outgrowth without neuronal cell death

(Mattson et al., 1988). We applied this model of glutamate-induced dendritic regression to examine the possible role of CD44 knockdown in preventing dendrite shortening. On day 2 after seeding, pyramidal neurons were transfected with either pSuper/GFP or CD44 shRNA/GFP plasmids. At 2 hours after transfection, the cells were exposed to glutamate (50 µM) for 3 days as described previously (Mattson et al., 1988). The cells were fixed on DIV5, and dendritic trees (Fig. 8A) were morphometrically analyzed. The TDL and TNDT of pSuper-transfected cells were significantly reduced by glutamate treatment (Fig. 8B,D). The Sholl analysis of neurons upon glutamate exposure revealed a downward shift of the plot compared with controls (Fig. 8C), indicating a decrease in the complexity of dendritic trees. The silencing of CD44 resulted in less pronounced growth inhibition of dendrites following glutamate treatment. Moreover, the protective effect of CD44 shRNA was not observed when the cells were co-transfected with constitutively active Src kinase.

DISCUSSION

In the present study, we document the temporal expression pattern and ultrastructural dendritic localization of the CD44 adhesion molecule in the postnatally developing rat brain. Using *in vitro* and *in vivo* knockdown approaches, we also identify a novel physiological function of CD44 – this protein plays a role

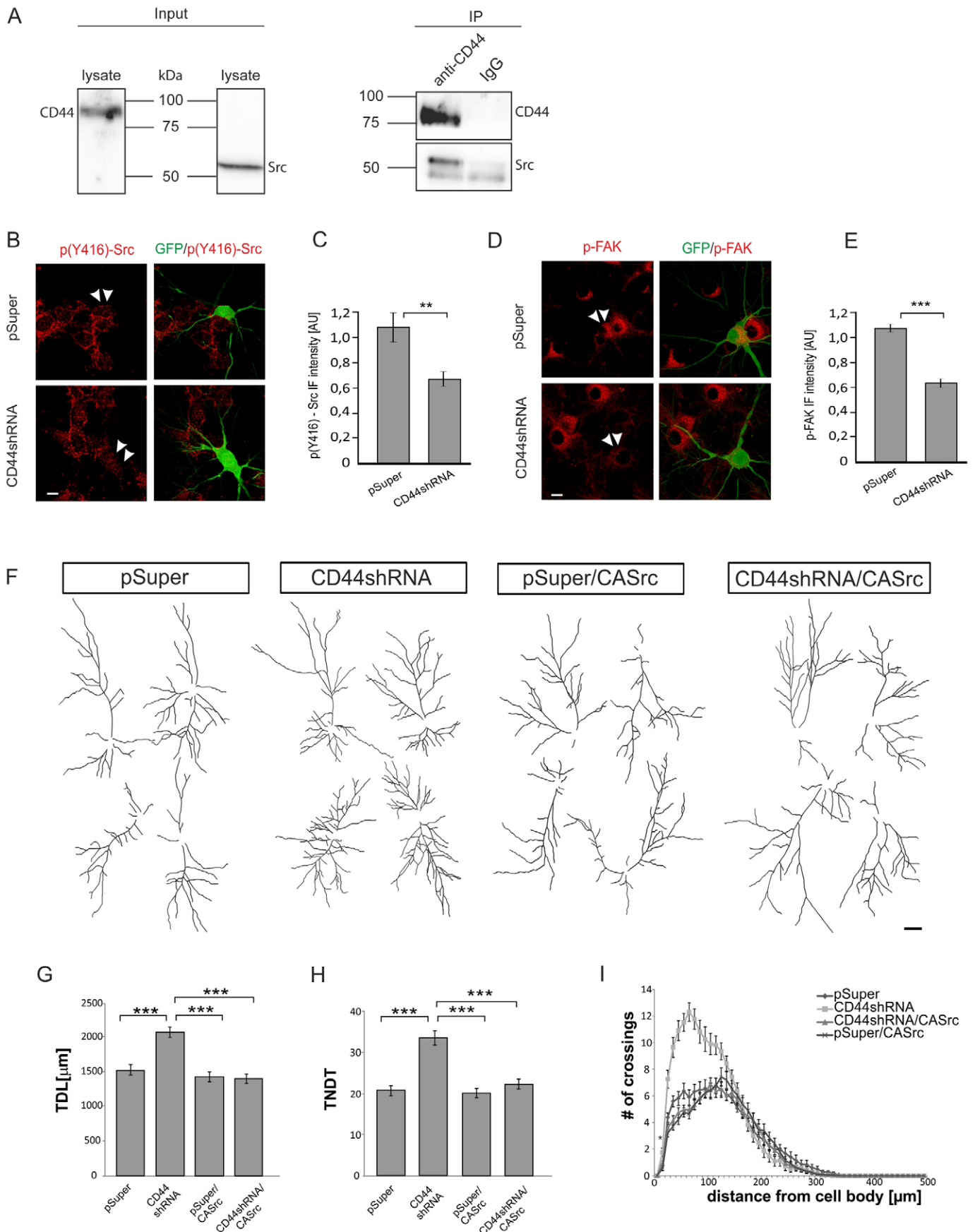


Fig. 6. See next page for legend.

Fig. 6. CD44 regulates the morphology of dendritic trees of hippocampal neurons by interacting with Src kinase and altering its activity. (A) Co-immunoprecipitation of endogenous CD44 and Src. Protein extracts (membrane fraction) of P10 rat hippocampi and cortex were analyzed for CD44 and Src expression (Input). A total of 1 mg of protein extract was subjected to immunoprecipitation (IP) with an antibody specific to CD44 or anti-IgG (negative control). Samples were then probed for precipitated CD44 and Src by western blotting. The data are representative of multiple independent experiments. (B–E) Primary hippocampal neurons transfected with pSuper or CD44 shRNA plasmids together with β -actin–GFP were subjected to immunocytochemistry using (B) anti-pY416-Src (red) or (D) anti-pY576-FAK (red) antibodies. Arrowheads indicate transfected cells. Scale bars: 10 μ m. Quantitative analysis of immunofluorescence (IF) intensity of (C) p-Src and (E) p-FAK in transfected cells. AU, arbitrary units. (F) Tracings of representative neurons co-transfected with pSuper, CD44 shRNA, CD44 shRNA/CASrc (Y527F) or pSuper/CASrc plasmids together with GFP-coding vector. Scale bar: 50 μ m. (G) Total dendritic length (TDL) and (H) total number of dendritic tips (TNDT) for neurons treated as in F. (I) Sholl analysis of hippocampal neurons after transfection with the indicated plasmids. $n=50$ neurons per group. At distances 10–150 μ m from the cell body, the differences between CD44 shRNA and the other groups were statistically significant. All quantitative data show the mean \pm s.e.m.; ** $P<0.01$; *** $P<0.001$.

in the regulation of neuronal morphology by restricting the elaboration of dendritic arbors. Our results clearly demonstrate that CD44 defines the structure of the Golgi, suggesting that CD44 might regulate dendritic arbor development by modulating Golgi morphology and positioning. Finally, we demonstrate that CD44 silencing decreases the glutamate-induced reduction of dendrite outgrowth. All of the effects observed herein upon CD44

knockdown are dependent on Src tyrosine kinase activity. Moreover, we show that the polymerization of actin filaments is crucial for the fragmentation of the Golgi induced by CD44 knockdown. Taken together, our findings uncover a novel cellular mechanism that is involved in the acquisition of proper neuronal morphology that might be a therapeutic target for disorders that involve dendritic pathology.

The majority of extracellular or transmembrane proteins that have been described to date as regulators of dendritogenesis have been shown to have a positive effect on dendritic growth (reviewed in Urbanska et al., 2008; Jan and Jan, 2010). Only a few such proteins have been shown to interfere with proper dendritic arbor formation by inhibiting its growth and branching. These include (1) a product of seizure-related gene 6 (SEZ-6; Gunnarsen et al., 2007), (2) the polysialylated form of the neural cell adhesion molecule (PSA-NCAM; McCall et al., 2013), (3) brain angiogenesis inhibitor 3 (BAI3; Lanoue et al., 2013) and (4) cadherin EGF LAG seven-pass G-type receptor 3 (CELSR-3; Shima et al., 2007). Growth-inhibitory mechanisms can play an important role in proper neuronal wiring, preventing excessive development of the neuronal network. Hyaluronan is one of the best-known growth- and regeneration-inhibiting molecules in the mammalian CNS (Mironova and Giger, 2013). Therefore, our findings that CD44, the main hyaluronan receptor, inhibits dendritogenesis provide new insights in this field.

The shape and localization of the Golgi in neurons are precisely related to their polar morphology. During the development of pyramidal neurons, the Golgi first localizes at

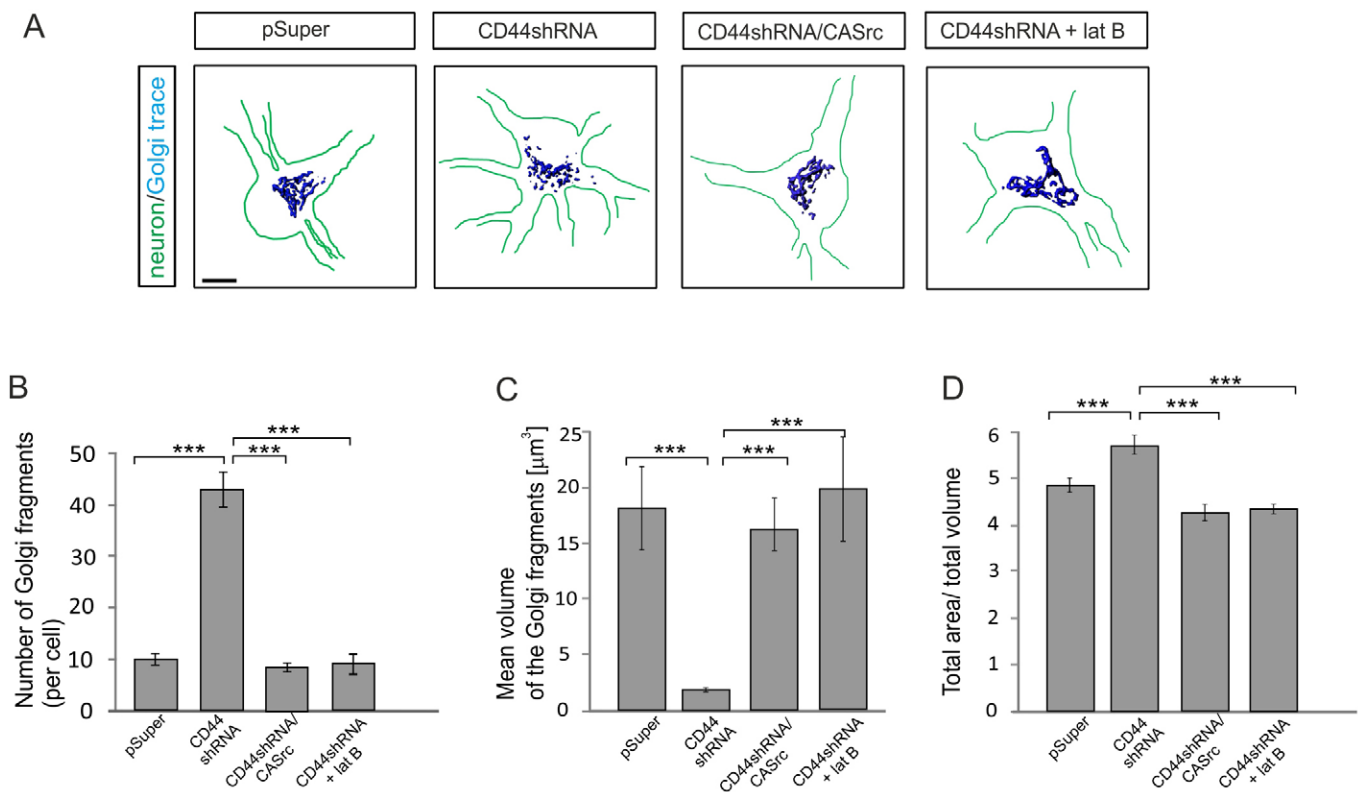


Fig. 7. CD44 knockdown-induced Golgi fragmentation is prevented by the activation of Src kinase and inhibition of actin polymerization. (A) Golgi three-dimensional reconstructions of GM130-labeled cultured hippocampal neurons transfected with pSuper, CD44 shRNA and CD44 shRNA/CASrc (Y527F) plasmids together with GFP-coding vector- or CD44 shRNA-transfected cells treated with latrunculin B (lat B). Scale bar: 10 μ m. Quantification of (B) the number of Golgi fragments, (C) the mean volume of the Golgi fragments and (D) the ratio of total surface area to total volume of the Golgi. Analyses of the Golgi of 40 cells per each experimental condition were performed. Data show the mean \pm s.e.m.; *** $P<0.001$.

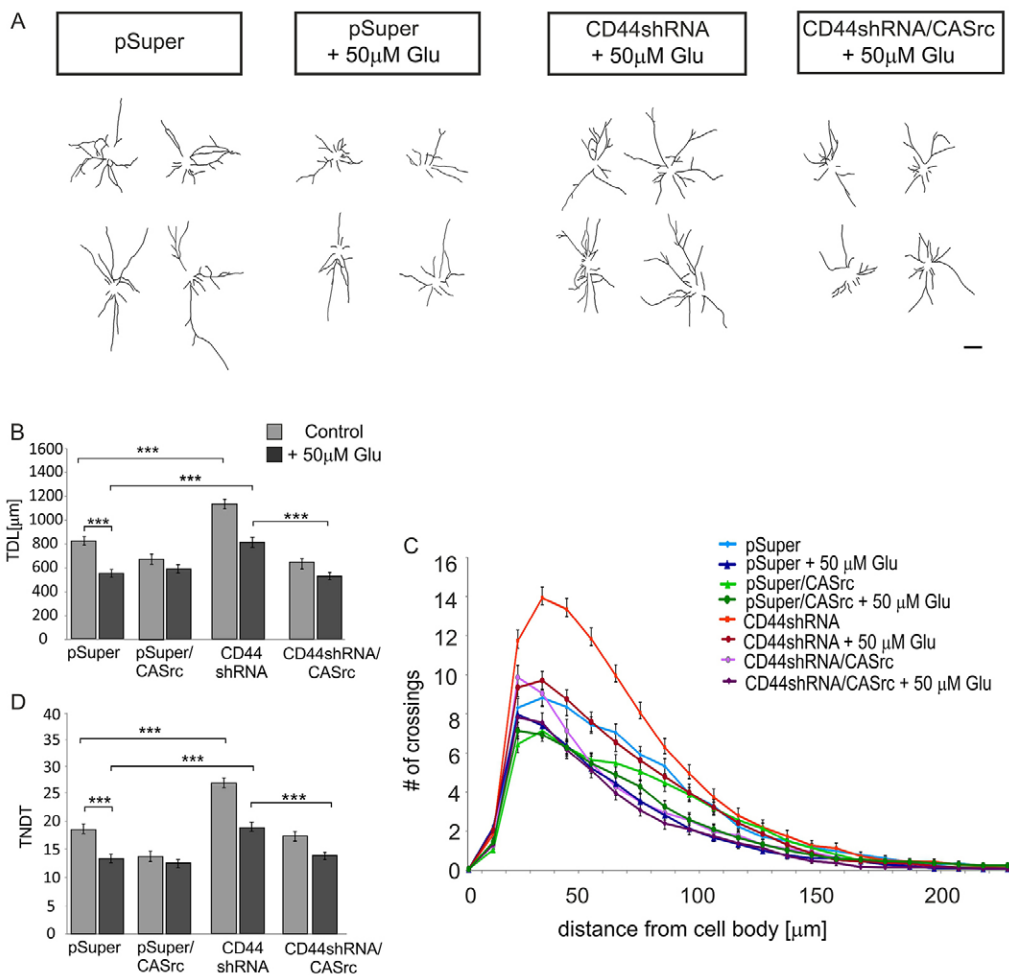


Fig. 8. Partial protective effect of CD44 knockdown on young hippocampal neurons treated with a subtoxic concentration of glutamate. Neurons were transfected with pSuper, CD44 shRNA, CD44 shRNA/CASrc (Y527F) or pSuper/CASrc plasmids together with GFP-coding vector on DIV2 and treated with 50 μm glutamate (Glu) for 3 days. Control neurons (non-treated) and glutamate-treated neurons were fixed on DIV5. (A) Tracings of representative neurons for all groups. Scale bar: 50 μm. (B) Total dendritic length (TDL) and (D) total number of dendritic tips (TNDT) for neurons treated as in A. (C) Sholl analysis of hippocampal neurons after transfection with the indicated plasmids. The detailed data of the statistical analysis are presented in supplementary material Tables S1–S3. Data show the mean \pm s.e.m. ($n=50$ neurons per group); *** $P<0.001$.

the axon emergence site, which becomes the future basal side (de Anda et al., 2005). It is subsequently positioned on the apical side (Horton et al., 2005), sending outposts into the longest, most complex dendrite. The outposts selectively localize to dendritic branch points. The morphology and function of the Golgi have been proposed to determine the formation of proper dendritic arbors through directional membrane trafficking, which is crucial for the growth and maintenance of dendritic processes (Sann et al., 2009). However, Ori-McKenney et al. recently demonstrated that the key function of Golgi outposts is to acentrosomally nucleate microtubules, thereby directly increasing dendritic arbor elaboration (Ori-McKenney et al., 2012). We found that the significant dispersion of the Golgi in neurons with elaborated dendritic trees was attributable to diminished CD44 expression. Such morphological rearrangement of the Golgi can provide more efficient acentrosomal microtubule growth, thus fostering the exaggerated complexity of the developing dendrite. Interestingly, the loss of CD44 *in vivo* had differential effects on the two types of pyramidal neuron dendrites, enhancing the branching of the basal dendrites, but not of the apical dendrites. Numerous mechanisms have been shown to regulate apical and basal dendrite outgrowth (Bi et al., 2001; Tran et al., 2009; Srivastava et al., 2012). Some of the mechanisms act selectively on apical or basal dendrites. Signaling of Sema3A through its receptor complex consisting of PlexA4 (also known as PLXNA4) and its co-receptor NP1 (also known as NRP1), for example, controls basal dendrite arborization in layer V cortical neurons

(Tran et al., 2009). Additionally, Sema3A and thousand-and-one-amino-acid 2 kinase (TAOK2) were shown to modulate the formation of basal dendrites through the activation of the c-Jun N-terminal kinase (JNK) (de Anda et al., 2012). By contrast, the Angelman's syndrome protein ubiquitin-protein ligase E3A (Ube3A) promotes apical dendrite outgrowth by regulating the asymmetric distribution of the Golgi (Miao et al., 2013). Our data, obtained *in vitro*, showing dispersed and hence less-polarized morphology of the Golgi following CD44 knockdown suggest that CD44 might regulate basal dendrite arborization by modulating the localization and function of the Golgi. It would also be interesting to investigate the molecular link of CD44 with the aforementioned molecular pathways involved in basal dendrite arborization. Remarkably, reversible Golgi fragmentation was recently observed in neurons upon increased neuronal activity (Thayer et al., 2013), demonstrating that Golgi dispersion can be a physiological response of neuronal cells to external stimuli. The possible relationships between this phenomenon and CD44-dependent fragmentation described herein remain to be determined.

The non-receptor tyrosine kinases Fyn, Lck and Src have been shown to interact with the intracellular domain of CD44 and initiate cytoskeleton reorganization in many cell types, including tumor cells and lymphocytes (Taher et al., 1996; Ilangumaran et al., 1998; Bourguignon et al., 2001; Lee et al., 2008; Bourguignon et al., 2010). In sensory neurons, CD44 inhibits the plasma membrane Ca^{2+} pump by activating tyrosine-kinase-dependent signaling

(Ghosh et al., 2011). Importantly, inhibitors of tyrosine kinases have been shown to potentiate substrate-induced neurite growth in neurons cultured *in vitro* (Bixby and Jhabvala, 1992; Williams et al., 1994). In the present study, we demonstrate that Src kinase directly interacts with CD44 in the rat brain and acts as a downstream effector of the CD44 molecule in the regulation of dendritic tree morphology. Moreover, our experiments indicate that CD44 influences Golgi morphology in a Src-dependent manner. We have found that Src activity restores the ‘normal’ non-fragmented morphology of the Golgi in neurons that have diminished CD44 expression. Constitutively active Src kinase does not influence the morphology of organelles in control cells. In contrast to our results, in non-neuronal cells, Src kinase activity has been shown to induce vesiculated cisternae of the Golgi (supplementary material Fig. S1; Weller et al., 2010). An opposite effect of CASrc expression in neuronal versus non-neuronal cells might be attributable to the differential expression levels of this mutant in these cells. In HeLa cells that were transfected with CASrc, the active form of Src was expressed at a much higher level than in neuronal cells (supplementary material Fig. S1). The contradictory consequence of Src activation observed in neuronal cells might also suggest that the effect of Src activity on Golgi morphology can be cell-type-specific and associated with a particular function of the Golgi in the arborization of pyramidal neurons. To further investigate the cellular mechanisms that are responsible for regulating Golgi morphology through the CD44–Src signaling pathway, we focused on remodeling the actin cytoskeleton. Src kinase and its downstream effectors are involved in regulating actin dynamics (Mitra et al., 2005). The interaction between the actin cytoskeleton and membrane trafficking appears to be directly involved in the biogenesis of Golgi-derived transport carriers and maintenance of the unique flat shape of Golgi cisternae (Egea et al., 2006). The force generated by actin polymerization has been proposed to be involved in the generation (i.e. budding and fission processes) of Golgi-derived vesicles (Egea et al., 2006). Moreover, the involvement of the Golgi protein GOLPH3, myosin Myo18A and F-actin in the generation of the tensile force on the Golgi that results in vesiculation has recently been reported (Dippold et al., 2009). The blockade of actin polymerization by latrunculin B reverses DNA-damage-induced Golgi dispersion in non-neuronal cells (Farber-Katz et al., 2014). In accordance with these findings, we show herein that latrunculin B reverses Golgi fragmentation induced by CD44 knockdown, indicating the existence of an actin-dependent mechanism associated with Golgi disassembly in neurons. We propose a model by which CD44 (by binding to Src kinase) induces Src kinase activation and subsequent phosphorylation of FAK kinase, which in turn phosphorylates its downstream substrates (e.g. α -actinin). This process consequently leads to a reduction in the crosslinking and polymerization of actin filaments and decreases the tension force exerted on the Golgi, thus preventing excessive vesiculation of the organelle. Collectively, our data suggest a novel morphogenetic pathway in neurons with the sequential involvement of CD44, Src, FAK, actin remodeling and the Golgi.

The alteration of dendrite morphology, including changes in dendrite branching patterns, the fragmentation of dendrites and the retraction or loss of dendrite branching, are implicated in several neurodegenerative and neurodevelopmental disorders (reviewed in Kulkarni and Firestein, 2012) and in brain injury. Unraveling the molecular mechanisms that are directed by positive and negative extracellular signals that regulate neurite outgrowth might provide new prospects for the treatment of such

brain diseases. Excitotoxicity, a form of neuronal damage caused by the excessive activation of glutamate receptors, is a neurotoxic mechanism that is implicated in the pathogenesis of many neurodegenerative disorders and in stroke (reviewed in Mattson and Sherman, 2003). In the present study, we apply an *in vitro* model of glutamate-induced damage (Mattson et al., 1988) that results in dendrite shortening without causing neuronal cell death. We show that CD44 shRNA partially prevents glutamate-induced dendrite shortening, and this protective effect depends on Src kinase inhibition. Our data are consistent with the observation that the lack of CD44 *in vivo* protects the brain from injury in a mouse model of cerebral ischemia (Wang et al., 2002). Moreover, inhibitors of Src kinases have been shown to exert protective effects on brain injury after stroke (Paul et al., 2001; Liang et al., 2009). Taken together, these data indicate that inhibition of the CD44–Src signaling pathway in neuronal cells might be considered therapeutically relevant for brain pathologies associated with dendritic tree impairment.

MATERIALS AND METHODS

Animals

The experiments were performed in Wistar rats of both sexes. All of the procedures were performed according to the rules established by the First Local Ethical Committee on Animal Research in Warsaw, based on national laws that are in full agreement with the European Union directive on animal experimentation.

Immunogold electron microscopy

The procedure was performed in P10 hippocampi as described previously (Wilczynski et al., 2008). For immunodetection, sheep polyclonal anti-CD44 (1:50; R&D Systems) followed by secondary antibodies coupled to 10-nm gold particles were applied (Electron Microscopy Sciences). Non-immune sheep IgG (BD Pharmingen) was used as a negative control. The gold particle densities within various ultrastructural compartments were measured in digital micrographs using ImageJ (National Institutes of Health, Bethesda, MD). The statistical evaluation of labeling was performed using the χ^2 test with regard to the observed and expected gold counts in the given compartments (Mayhew and Lucocq, 2008).

Western blotting

The procedure was performed in hippocampal or cortical extracts from rats that were sacrificed on E18 or P3–P60, or extracts from cell cultures as described previously (Dzwonek et al., 2009). The following antibodies were used: sheep anti-CD44 (R&D Systems), rabbit anti-GFP (MBL International), chicken anti- β -galactosidase (Abcam), mouse anti-GAPDH (Millipore) and anti-Src (Cell Signaling). The densitometry analysis of three independent western blots was performed using ImageJ software, and the protein level was designated as 1 in the control (pSuper) group. All of the western blot densitometry data were normalized to the loading control, GAPDH.

In vivo electroporation

Postnatal iontoporation was performed as described recently (De la Rossa et al., 2013), with modifications. P1 pups were anesthetized on ice for 5 minutes and injected with 1 μ l of DNA (3 μ g μ l⁻¹) directly into the cerebral cortex using a 30- μ m-tip glass micropipette. Prior to injection, the plasmid solution was mixed with 1 μ l of TCHD (100 mg ml⁻¹) to enhance nuclear membrane permeability. Electroporation was performed in a Nepagene WY21 apparatus at 4 minutes after the injection with two trains of six pulses (80 V, 50-ms duration) delivered through 5-mm electrode paddles that were placed on each side of the skull.

DNA constructs

The following mammalian expression plasmids have been described previously: pSuper vector (Brummelkamp et al., 2002), β -actin-GFP (Jaworski et al., 2005), β -actin-RFP (Hoogenraad et al., 2007), EF α - β -gal

(Konopka et al., 2005) and pLNCX chick src Y527F (constitutively active Src; Addgene plasmid 13660; <http://www.addgene.org/13660/>). The rat CD44 full-length coding sequence (standard form; GenBank BC127485.1) was amplified by PCR using total mRNA that was isolated from the rat hippocampus as a template with the primers 5'-CTGAATTCGACAAGGTTTGGTGGCAC-3' (forward) and 5'-CGTCGACTGCACCCCAATCTTCATATC-3' (reverse). The product was cloned into *EcoRI/SalI* restriction sites of the β -actin GFP plasmid. CD44 shRNA sequences were designed against rat CD44 mRNA (NM_012924), targeting the sequences 2075–2097 (CD44 shRNA #1963) and 202–224 (CD44 shRNA #90) within the coding sequence. Oligomers that encoded these shRNAs were next introduced into the pSuper plasmid. CD44-GFP shRNA-resistant forms (CD44Rescue) were generated using the QuikChange Site-Directed Mutagenesis Kit (Stratagene).

Cell cultures

HEK293 and HeLa cell cultures and their transfection were performed as described previously (Percy et al., 2011). Primary rat hippocampal cultures were prepared from P0 rat brains as described previously (Michaluk et al., 2011) and transfected using Lipofectamine 2000 (Invitrogen).

Immunofluorescence

The procedures were performed in cultured neurons or tissue sections as described previously (Wilczynski et al., 2008; Urbanska et al., 2012). The following primary antibodies were used in cells: sheep anti-CD44 antibody (1:500; R&D), mouse anti-GM130 (1:500; BD Bioscience), rabbit anti-pY416-Src (1:100; Cell Signaling), rabbit anti-pY576-FAK (1:100; Invitrogen), donkey anti-mouse-IgG conjugated to DyLight 649 and donkey anti-rabbit-IgG conjugated to CY3 (Jackson ImmunoResearch). The following primary antibodies were used in sections: sheep anti-CD44 (1:200; R&D), mouse anti-MAP-2 (1:200; Sigma-Aldrich) and chicken anti-GFAP (1:200; Abcam). The following secondary antibodies were used: anti-mouse-IgG conjugated to DyLight 546, anti-chicken-IgG conjugated to DyLight 649 and anti-sheep-IgG conjugated to DyLight 488 (all from donkey, diluted 1:500; Jackson ImmunoResearch). Nuclei were counterstained with DAPI (Vectashield Mounting Medium with DAPI, Vector Labs). Fluorescent Nissl staining was performed according to the manufacturer's protocol (Life Technologies).

Immunoprecipitation

Co-immunoprecipitation from the hippocampus and cortex was performed as described previously (Renner et al., 2012). Briefly, brain samples were isolated from P10 Wistar rats and homogenized, and membrane fractions were prepared. Lysates were incubated with a sheep-anti-CD44 antibody (R&D Systems) or sheep anti-IgG isotype control overnight at 4°C, followed by incubation with Protein-A–Sephacel, SDS-PAGE and western blotting with rabbit polyclonal antibody directed against Src (Cell Signaling Technology).

Image acquisition and analysis

For the analysis of dendritic morphology, cell images were obtained with a Nikon fluorescence microscope with a 20 \times objective. Morphometric analyses were performed using ImageJ with NeuronJ (Meijering et al., 2004) and the Sholl plug-in (Percy et al., 2011). Fluorescently labeled cells and brain sections were examined under a Leica TCS SP5 or Zeiss LSM 780 confocal microscope. The analysis of the average immunofluorescence intensity of CD44, phosphorylated Src and phosphorylated FAK was performed using ImageJ software. The intensity of fluorescence in transfected cells was normalized to the intensity of non-transfected adjacent cells. For the Golgi analysis, the images of the immunofluorescently labeled cells were acquired on a Zeiss LSM 780 confocal microscope with z-stacks of 0.25 μ m. Imaris software was used for three-dimensional reconstruction and quantification of the number of distinct Golgi fragments and the volume and surface area analysis of the fragments, as described

previously (Thayer et al., 2013). The ratio of the total surface area of the Golgi to the total volume of the Golgi per cell was calculated as an additional parameter to describe Golgi dispersion.

Latrunculin B treatment

Neurons were transfected on DIV5 with pSuper or CD44 shRNA plasmids. At 24 hours later, the cells were incubated with latrunculin B (2.5 μ M) for 24 hours. Cells were fixed on DIV7.

Glutamate treatment

Hippocampal neurons were transfected on DIV2 with plasmids (β -actin GFP, pSuper, CD44 shRNA and CASrc as indicated in Fig. 8). At 2 hours after transfection, the cell medium was changed, and the cells were exposed to 50 μ M glutamate for 3 days (Mattson et al., 1988).

Statistical analyses

The data were obtained from three independent batches of neurons. The data are expressed as mean values and standard error of the mean and were analyzed using one-way analysis of variance (ANOVA) followed by Dunnett's C or Sidak post-hoc tests, depending on whether the assumption of homogeneity of variance was met. For the statistical analysis of the Sholl results, we used a univariate mixed-model ANOVA followed by the Bonferroni post-hoc test. The statistical analyses were performed using Statistica software (StatSoft).

Acknowledgements

We thank Krishnendu Ganguly (Nencki Institute of Experimental Biology, Warsaw, Poland) for experimental assistance. We thank Tomek Prószyński (Nencki Institute of Experimental Biology, Warsaw, Poland) and Joan Brugge (Harvard Medical School, Boston, MA) for sharing the plasmids from the Addgene plasmid repository.

Competing interests

The authors declare no competing interests.

Author contributions

J.D. designed and performed the experiments and analyzed the data. A.S., A.K., P.T. and M.B. performed the experiments and analyzed the data. J.L. and A.G. performed the experiments. J.J., L.S., H.D., I.F. and E.P. contributed new reagents/analytic tools. J.W., J.J. and G.M.W. analyzed the data. J.D. and G.M.W. wrote the paper. J.D. supervised the project.

Funding

This research was supported by a Foundation for Polish Science PARENT-BRIDGE grant, co-financed by the European Union Regional Development Fund [grant number PARENT-BRIDGE/2011-3/2]. G.M.W. was supported by the National Science Centre [grant number 7873/B/P01/2011/40]; and a grant from the European Regional Development Fund under the Operational Program Innovative Economy [grant number POIG 01.01.02-00-008/08]. J.W. was supported by the National Science Centre [grant number DEC-2012/06/M/NZ3/00163].

Supplementary material

Supplementary material available online at <http://jcs.biologists.org/lookup/suppl/doi:10.1242/jcs.154542/-DC1>

References

- Bi, X., Lynch, G., Zhou, J. and Gall, C. M. (2001). Polarized distribution of alpha5 integrin in dendrites of hippocampal and cortical neurons. *J. Comp. Neurol.* **435**, 184–193.
- Bixby, J. L. and Jhabvala, P. (1992). Inhibition of tyrosine phosphorylation potentiates substrate-induced neurite growth. *J. Neurobiol.* **23**, 468–480.
- Bourguignon, L. Y. (2008). Hyaluronan-mediated CD44 activation of RhoGTPase signaling and cytoskeleton function promotes tumor progression. *Semin. Cancer Biol.* **18**, 251–259.
- Bourguignon, L. Y., Zhu, H., Shao, L. and Chen, Y. W. (2001). CD44 interaction with c-Src kinase promotes cortactin-mediated cytoskeleton function and hyaluronan acid-dependent ovarian tumor cell migration. *J. Biol. Chem.* **276**, 7327–7336.
- Bourguignon, L. Y., Wong, G., Earle, C., Krueger, K. and Spevak, C. C. (2010). Hyaluronan-CD44 interaction promotes c-Src-mediated twist signaling, microRNA-10b expression, and RhoA/RhoC up-regulation, leading to Rho-kinase-associated cytoskeleton activation and breast tumor cell invasion. *J. Biol. Chem.* **285**, 36721–36735.

- Bouvier-Labit, C., Liprandi, A., Monti, G., Pellissier, J. F. and Figarella-Branger, D. (2002). CD44H is expressed by cells of the oligodendrocyte lineage and by oligodendrogliomas in humans. *J. Neurooncol.* **60**, 127–134.
- Brummelkamp, T. R., Bernards, R. and Agami, R. (2002). A system for stable expression of short interfering RNAs in mammalian cells. *Science* **296**, 550–553.
- de Anda, F. C., Pollarolo, G., Da Silva, J. S., Camoletto, P. G., Feiguin, F. and Dotti, C. G. (2005). Centrosome localization determines neuronal polarity. *Nature* **436**, 704–708.
- de Anda, F. C., Rosario, A. L., Durak, O., Tran, T., Gräff, J., Meletis, K., Rei, D., Soda, T., Madabhushi, R., Ginty, D. D. et al. (2012). Autism spectrum disorder susceptibility gene TAOK2 affects basal dendrite formation in the neocortex. *Nat. Neurosci.* **15**, 1022–1031.
- De la Rossa, A., Bellone, C., Golding, B., Vitali, I., Moss, J., Toni, N., Lüscher, C. and Jabaudon, D. (2013). In vivo reprogramming of circuit connectivity in postmitotic neocortical neurons. *Nat. Neurosci.* **16**, 193–200.
- Dippold, H. C., Ng, M. M., Farber-Katz, S. E., Lee, S. K., Kerr, M. L., Peterman, M. C., Sim, R., Wiharto, P. A., Galbraith, K. A., Madhavarapu, S. et al. (2009). GOLPH3 bridges phosphatidylinositol-4-phosphate and actomyosin to stretch and shape the Golgi to promote budding. *Cell* **139**, 337–351.
- Dzwonek, J., Preobrazhenska, O., Cazzola, S., Conidi, A., Schellens, A., van Dinther, M., Stubbs, A., Klippel, A., Huylebroeck, D., ten Dijke, P. et al. (2009). Smad3 is a key nonredundant mediator of transforming growth factor beta signaling in Nme mouse mammary epithelial cells. *Mol. Cancer Res.* **7**, 1342–1353.
- Egea, G., Lázaro-Díéguez, F. and Vilella, M. (2006). Actin dynamics at the Golgi complex in mammalian cells. *Curr. Opin. Cell Biol.* **18**, 168–178.
- Farber-Katz, S. E., Dippold, H. C., Buschman, M. D., Peterman, M. C., Xing, M., Noakes, C. J., Tat, J., Ng, M. M., Rahajeng, J., Cowan, D. M. et al. (2014). DNA damage triggers Golgi dispersal via DNA-PK and GOLPH3. *Cell* **156**, 413–427.
- Ghosh, B., Li, Y. and Thayer, S. A. (2011). Inhibition of the plasma membrane Ca²⁺ pump by CD44 receptor activation of tyrosine kinases increases the action potential afterhyperpolarization in sensory neurons. *J. Neurosci.* **31**, 2361–2370.
- Girgrah, N., Letarte, M., Becker, L. E., Cruz, T. F., Theriault, E. and Moscarello, M. A. (1991). Localization of the CD44 glycoprotein to fibrous astrocytes in normal white matter and to reactive astrocytes in active lesions in multiple sclerosis. *J. Neuropathol. Exp. Neurol.* **50**, 779–792.
- Glezer, I., Bittencourt, J. C. and Rivest, S. (2009). Neuronal expression of Cd36, Cd44, and Cd83 antigen transcripts maps to distinct and specific murine brain circuits. *J. Comp. Neurol.* **517**, 906–924.
- Gorlewicz, A., Włodarczyk, J., Wilczek, E., Gawlak, M., Cabaj, A., Majczynski, H., Nestorowicz, K., Herbiak, M. A., Grieb, P., Slawinska, U. et al. (2009). CD44 is expressed in non-myelinating Schwann cells of the adult rat, and may play a role in neurodegeneration-induced glial plasticity at the neuromuscular junction. *Neurobiol. Dis.* **34**, 245–258.
- Gulledge, A. T., Kampa, B. M. and Stuart, G. J. (2005). Synaptic integration in dendritic trees. *J. Neurobiol.* **64**, 75–90.
- Gunnersen, J. M., Kim, M. H., Fuller, S. J., De Silva, M., Britto, J. M., Hammond, V. E., Davies, P. J., Petrou, S., Faber, E. S., Sah, P. et al. (2007). Seiz-6 proteins affect dendritic arborization patterns and excitability of cortical pyramidal neurons. *Neuron* **56**, 621–639.
- Hanks, S. K., Ryzhova, L., Shin, N. Y. and Brábek, J. (2003). Focal adhesion kinase signaling activities and their implications in the control of cell survival and motility. *Front. Biosci.* **8**, d982–d996.
- Hoogenraad, C. C., Feliu-Mojer, M. I., Spangler, S. A., Milstein, A. D., Dunah, A. W., Hung, A. Y. and Sheng, M. (2007). Liprinalpha1 degradation by calcium/calmodulin-dependent protein kinase II regulates LAR receptor tyrosine phosphatase distribution and dendrite development. *Dev. Cell* **12**, 587–602.
- Horton, A. C., Rác, B., Monson, E. E., Lin, A. L., Weinberg, R. J. and Ehlers, M. D. (2005). Polarized secretory trafficking directs cargo for asymmetric dendrite growth and morphogenesis. *Neuron* **48**, 757–771.
- Ilangumaran, S., Briol, A. and Hoessli, D. C. (1998). CD44 selectively associates with active Src family protein tyrosine kinases Lck and Fyn in glycosphingolipid-rich plasma membrane domains of human peripheral blood lymphocytes. *Blood* **91**, 3901–3908.
- Jan, Y. N. and Jan, L. Y. (2010). Branching out: mechanisms of dendritic arborization. *Nat. Rev. Neurosci.* **11**, 316–328.
- Jaworski, J., Spangler, S., Seeburg, D. P., Hoogenraad, C. C. and Sheng, M. (2005). Control of dendritic arborization by the phosphoinositide-3-kinase-Akt-mammalian target of rapamycin pathway. *J. Neurosci.* **25**, 11300–11312.
- Jones, L. L., Kreutzberg, G. W. and Raivich, G. (1997). Regulation of CD44 in the regenerating mouse facial motor nucleus. *Eur. J. Neurosci.* **9**, 1854–1863.
- Kaaijk, P., Pals, S. T., Morsink, F., Bosch, D. A. and Troost, D. (1997). Differential expression of CD44 splice variants in the normal human central nervous system. *J. Neuroimmunol.* **73**, 70–76.
- Kaufmann, W. E. and Moser, H. W. (2000). Dendritic anomalies in disorders associated with mental retardation. *Cereb. Cortex* **10**, 981–991.
- Koleske, A. J. (2013). Molecular mechanisms of dendrite stability. *Nat. Rev. Neurosci.* **14**, 536–550.
- Konopka, W., Duniec, K., Mioduszevska, B., Proszynski, T., Jaworski, J. and Kaczmarek, L. (2005). hCMV and Tet promoters for inducible gene expression in rat neurons in vitro and in vivo. *Neurobiol. Dis.* **19**, 283–292.
- Kulkarni, V. A. and Firestein, B. L. (2012). The dendritic tree and brain disorders. *Mol. Cell. Neurosci.* **50**, 10–20.
- Lanoue, V., Usardi, A., Sigoillot, S. M., Talleur, M., Iyer, K., Mariani, J., Isope, P., Vojdani, G., Heintz, N. and Selimi, F. (2013). The adhesion-GPCR BAI3, a gene linked to psychiatric disorders, regulates dendrite morphogenesis in neurons. *Mol. Psychiatry* **18**, 943–950.
- Lázaro-Díéguez, F., Jiménez, N., Barth, H., Koster, A. J., Renau-Piqueras, J., Llopis, J. L., Burger, K. N. and Egea, G. (2006). Actin filaments are involved in the maintenance of Golgi cisternae morphology and intra-Golgi pH. *Cell Motil. Cytoskeleton* **63**, 778–791.
- Lee, J. L., Wang, M. J., Sudhir, P. R. and Chen, J. Y. (2008). CD44 engagement promotes matrix-derived survival through the CD44-SRC-integrin axis in lipid rafts. *Mol. Cell. Biol.* **28**, 5710–5723.
- Liang, S., Pong, K., Gonzales, C., Chen, Y., Ling, H. P., Mark, R. J., Boschelli, F., Boschelli, D. H., Ye, F., Barrios Sosa, A. C. et al. (2009). Neuroprotective profile of novel SRC kinase inhibitors in rodent models of cerebral ischemia. *J. Pharmacol. Exp. Ther.* **331**, 827–835.
- Lin, L. and Chan, S. O. (2003). Perturbation of CD44 function affects chiasmatic routing of retinal axons in brain slice preparations of the mouse retinofugal pathway. *Eur. J. Neurosci.* **17**, 2299–2312.
- Martin, T. A., Harrison, G., Mansel, R. E. and Jiang, W. G. (2003). The role of the CD44/ezrin complex in cancer metastasis. *Crit. Rev. Oncol. Hematol.* **46**, 165–186.
- Mattson, M. P. and Sherman, M. (2003). Perturbed signal transduction in neurodegenerative disorders involving aberrant protein aggregation. *Neuromolecular Med.* **4**, 109–132.
- Mattson, M. P., Dou, P. and Kater, S. B. (1988). Outgrowth-regulating actions of glutamate in isolated hippocampal pyramidal neurons. *J. Neurosci.* **8**, 2087–2100.
- Matzke, A., Sargsyan, V., Holtmann, B., Aramuni, G., Asan, E., Sendtner, M., Pace, G., Howells, N., Zhang, W., Ponta, H. et al. (2007). Haploinsufficiency of c-Met in cd44^{-/-} mice identifies a collaboration of CD44 and c-Met in vivo. *Mol. Cell. Biol.* **27**, 8797–8806.
- Mayhew, T. M. and Lucocq, J. M. (2008). Developments in cell biology for quantitative immunoelectron microscopy based on thin sections: a review. *Histochem. Cell Biol.* **130**, 299–313.
- McCall, T., Weil, Z. M., Nacher, J., Bloss, E. B., El Maarouf, A., Rutishauser, U. and McEwen, B. S. (2013). Depletion of polysialic acid from neural cell adhesion molecule (PSA-NCAM) increases CA3 dendritic arborization and increases vulnerability to excitotoxicity. *Exp. Neurol.* **241**, 5–12.
- Meijering, E., Jacob, M., Sarría, J. C., Steiner, P., Hirling, H. and Unser, M. (2004). Design and validation of a tool for neurite tracing and analysis in fluorescence microscopy images. *Cytometry A* **58A**, 167–176.
- Miao, S., Chen, R., Ye, J., Tan, G. H., Li, S., Zhang, J., Jiang, Y. H. and Xiong, Z. Q. (2013). The Angelman syndrome protein Ube3a is required for polarized dendrite morphogenesis in pyramidal neurons. *J. Neurosci.* **33**, 327–333.
- Michaluk, P., Wawrzyniak, M., Alot, P., Szczot, M., Wyrembek, P., Mercik, K., Medvedev, N., Wilczek, E., De Roo, M., Zuschratter, W. et al. (2011). Influence of matrix metalloproteinase MMP-9 on dendritic spine morphology. *J. Cell Sci.* **124**, 3369–3380.
- Mironova, Y. A. and Giger, R. J. (2013). Where no synapses go: gatekeepers of circuit remodeling and synaptic strength. *Trends Neurosci.* **36**, 363–373.
- Mitra, S. K., Hanson, D. A. and Schlaepfer, D. D. (2005). Focal adhesion kinase: in command and control of cell motility. *Nat. Rev. Mol. Cell Biol.* **6**, 56–68.
- Moretto, G., Xu, R. Y. and Kim, S. U. (1993). CD44 expression in human astrocytes and oligodendrocytes in culture. *J. Neuropathol. Exp. Neurol.* **52**, 419–423.
- Naruse, M., Shibasaki, K., Yokoyama, S., Kurachi, M. and Ishizaki, Y. (2013). Dynamic changes of CD44 expression from progenitors to subpopulations of astrocytes and neurons in developing cerebellum. *PLoS ONE* **8**, e53109.
- Novak, U. and Kaye, A. H. (2000). Extracellular matrix and the brain: components and function. *J. Clin. Neurosci.* **7**, 280–290.
- Ori-McKenney, K. M., Jan, L. Y. and Jan, Y. N. (2012). Golgi outposts shape dendrite morphology by functioning as sites of centrosomal microtubule nucleation in neurons. *Neuron* **76**, 921–930.
- Orian-Rousseau, V., Chen, L., Sleeman, J. P., Herrlich, P. and Ponta, H. (2002). CD44 is required for two consecutive steps in HGF/c-Met signaling. *Genes Dev.* **16**, 3074–3086.
- Paul, R., Zhang, Z. G., Eliceiri, B. P., Jiang, Q., Boccia, A. D., Zhang, R. L., Chopp, M. and Chereshe, D. A. (2001). Src deficiency or blockade of Src activity in mice provides cerebral protection following stroke. *Nat. Med.* **7**, 222–227.
- Percy, M., Urbanska, A. S., Krawczyk, P. S., Parobczak, K. and Jaworski, J. (2011). Zipcode binding protein 1 regulates the development of dendritic arbors in hippocampal neurons. *J. Neurosci.* **31**, 5271–5285.
- Ponta, H., Sherman, L. and Herrlich, P. A. (2003). CD44: from adhesion molecules to signalling regulators. *Nat. Rev. Mol. Cell Biol.* **4**, 33–45.
- Renner, U., Zeug, A., Woehler, A., Niebert, M., Dityatev, A., Dityateva, G., Gorinski, N., Guseva, D., Abdel-Galil, D., Fröhlich, M. et al. (2012). Heterodimerization of serotonin receptors 5-HT1A and 5-HT7 differentially regulates receptor signalling and trafficking. *J. Cell Sci.* **125**, 2486–2499.
- Ries, A., Goldberg, J. L. and Grimpe, B. (2007). A novel biological function for CD44 in axon growth of retinal ganglion cells identified by a bioinformatics approach. *J. Neurochem.* **103**, 1491–1505.
- Sann, S., Wang, Z., Brown, H. and Jin, Y. (2009). Roles of endosomal trafficking in neurite outgrowth and guidance. *Trends Cell Biol.* **19**, 317–324.
- Segev, I. and London, M. (2000). Untangling dendrites with quantitative models. *Science* **290**, 744–750.

- Sherman, L. S., Rizvi, T. A., Karyala, S. and Ratner, N. (2000). CD44 enhances neuregulin signaling by Schwann cells. *J. Cell Biol.* **150**, 1071-1084.
- Shima, Y., Kawaguchi, S. Y., Kosaka, K., Nakayama, M., Hoshino, M., Nabeshima, Y., Hirano, T. and Uemura, T. (2007). Opposing roles in neurite growth control by two seven-pass transmembrane cadherins. *Nat. Neurosci.* **10**, 963-969.
- Sretavan, D. W., Feng, L., Puré, E. and Reichardt, L. F. (1994). Embryonic neurons of the developing optic chiasm express L1 and CD44, cell surface molecules with opposing effects on retinal axon growth. *Neuron* **12**, 957-975.
- Srivastava, D. P., Woolfrey, K. M., Jones, K. A., Anderson, C. T., Smith, K. R., Russell, T. A., Lee, H., Yasvoina, M. V., Wokosin, D. L., Ozdinler, P. H. et al. (2012). An autism-associated variant of Epac2 reveals a role for Ras/Epac2 signaling in controlling basal dendrite maintenance in mice. *PLoS Biol.* **10**, e1001350.
- Taher, T. E., Smit, L., Griffioen, A. W., Schilder-Tol, E. J., Borst, J. and Pals, S. T. (1996). Signaling through CD44 is mediated by tyrosine kinases. Association with p56lck in T lymphocytes. *J. Biol. Chem.* **271**, 2863-2867.
- Thayer, D. A., Jan, Y. N. and Jan, L. Y. (2013). Increased neuronal activity fragments the Golgi complex. *Proc. Natl. Acad. Sci. USA* **110**, 1482-1487.
- Tran, T. S., Rubio, M. E., Clem, R. L., Johnson, D., Case, L., Tessier-Lavigne, M., Hagan, R. L., Ginty, D. D. and Kolodkin, A. L. (2009). Secreted semaphorins control spine distribution and morphogenesis in the postnatal CNS. *Nature* **462**, 1065-1069.
- Urbanska, M., Blazejczyk, M. and Jaworski, J. (2008). Molecular basis of dendritic arborization. *Acta Neurobiol. Exp. (Warsz.)* **68**, 264-288.
- Urbanska, M., Gozdz, A., Swiech, L. J. and Jaworski, J. (2012). Mammalian target of rapamycin complex 1 (mTORC1) and 2 (mTORC2) control the dendritic arbor morphology of hippocampal neurons. *J. Biol. Chem.* **287**, 30240-30256.
- Vogel, H., Butcher, E. C. and Picker, L. J. (1992). H-CAM expression in the human nervous system: evidence for a role in diverse glial interactions. *J. Neurocytol.* **21**, 363-373.
- Wang, X., Xu, L., Wang, H., Zhan, Y., Puré, E. and Feuerstein, G. Z. (2002). CD44 deficiency in mice protects brain from cerebral ischemia injury. *J. Neurochem.* **83**, 1172-1179.
- Weller, S. G., Capitani, M., Cao, H., Micaroni, M., Luini, A., Sallese, M. and McNiven, M. A. (2010). Src kinase regulates the integrity and function of the Golgi apparatus via activation of dynamin 2. *Proc. Natl. Acad. Sci. USA* **107**, 5863-5868.
- Wilczynski, G. M., Konopacki, F. A., Wilczek, E., Lasińska, Z., Gorlewicz, A., Michaluk, P., Wawrzyniak, M., Malinowska, M., Okulski, P., Kolodziej, L. R. et al. (2008). Important role of matrix metalloproteinase 9 in epileptogenesis. *J. Cell Biol.* **180**, 1021-1035.
- Williams, E. J., Walsh, F. S. and Doherty, P. (1994). Tyrosine kinase inhibitors can differentially inhibit integrin-dependent and CAM-stimulated neurite outgrowth. *J. Cell Biol.* **124**, 1029-1037.